

Effects of annealing on structural and magnetic properties of template synthesized cobalt nanowires useful as data storage and nano devices

Deepak Saini · R. P. Chauhan · Sanjeev Kumar

Received: 6 September 2013 / Accepted: 17 October 2013 / Published online: 27 October 2013
© Springer Science+Business Media New York 2013

Abstract Cobalt nanowires of 100 nm diameter were synthesised electrochemically, in the pores of anodic alumina membrane (AAM). Electrochemical impedance spectroscopy was used to study the in situ growth of cobalt nanowires in the AAM. The structural and morphological characterization of template synthesized cobalt nanowires was done through X-ray diffractometer and scanning electron microscope, respectively. Effect of annealing on electrical and magnetic properties of cobalt nanowires was also investigated.

1 Introduction

Magnetic nanowires (NWs) have the capability to fulfil the needs of today's technological demands like high density data storage devices, microwave devices and reprogrammable magnonic crystals etc. [1–3]. Cobalt NWs are one of the mostly investigated nanowires because of their fascinating structure property correlation. Usually two allotropic forms are exhibited by cobalt, i.e., face centered cubic (α -Co) phase and hexagonal close packed (ϵ -Co) phase. It is reported that the magnetic properties of

hexagonal close packed Co nanostructures can be customized through variation of structural properties, like crystallinity and orientation of its *c*-axis in the NWs [4].

In concurrence with shape anisotropy, the strong uniaxial magneto crystalline anisotropy along *c*-axis, acquires a partly controllable effective anisotropy of the NWs array [4]. Reports are available regarding dependence of phase and orientation of electrodeposited cobalt NWs on deposition parameters like current density, bath concentration, pH and magnetic field applied during deposition [5–10]. During the electrodeposition process, deposition of Co atoms at the cathode from the bath containing Co^{2+} ions involves the movement of Co^{2+} ions from bulk solution to the solution-cathode interface which consequently gets adsorbed on the cathode surface. In this technique, the mass-transport process is restricted by the diameter and length of the pores in the alumina template. Inside the nanopores, mass transport is limited by diffusion [11]. Usually, during the electrodeposition of less noble metal, hydrogen evolution occurs at the cathode. The occurrence of hydrogen gas evolution during the cobalt ion's deposition, influence the nucleation and growth of cobalt atoms. As a result, they should play a key role in defining the texture and phase of electrodeposited cobalt nanowires.

Nanowires have two quantum-confined dimensions and one unconfined dimension. Consequently, the electrical conduction behaviour of nanowires is dissimilar from that of their bulk counterpart [12–14]. In nanowires, due to their high density of electronic state, diameter-dependent band gap, enhanced surface scattering of electrons and phonons, increased excitation binding energy, high surface to volume ratio and large aspect ratio, nanowires of metals and semiconductors demonstrate exceptional electrical, magnetic, optical, thermoelectric and chemical properties compared to their bulk parent counterparts. In the present

D. Saini · S. Kumar (✉)
University College of Engineering, Punjabi University,
Patiala 147002, India
e-mail: sanjeevace_phy@yahoo.co.in;
sanjeev04101977@gmail.com

R. P. Chauhan
Department of Physics, National Institute of Technology,
Kurukshetra 136119, India

S. Kumar
Department of Applied Science, PEC University of Technology,
Chandigarh 160012, India

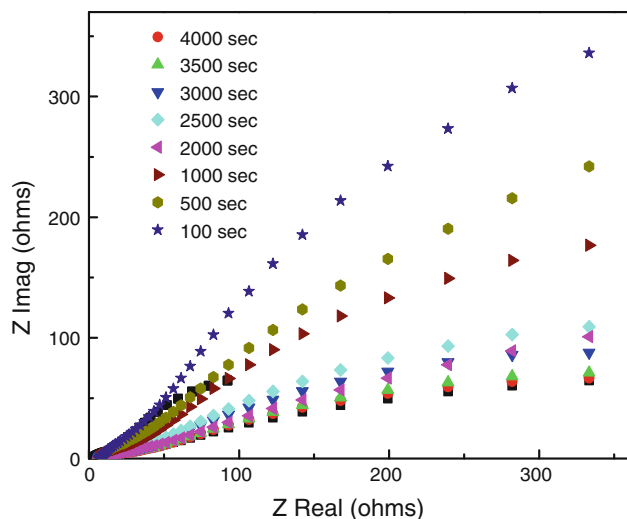


Fig. 1 Nyquist plots obtained with the AAM template electrode at different stages of the Co nanowires electrodeposition process at room temperature

paper, we reported the synthesis of cobalt nanowires using “template synthesis” technique [15–18] and the effect of annealing on their structural, electrical and magnetic properties.

2 Experimental

Template synthesis method was used for the synthesis of cobalt nanowires. AAM with pore diameter of 100 nm was used as template. 1 M cobalt sulphate dissolved in distilled water is used as electrolyte with some drops of H_2SO_4 . Three electrode system (Gamry reference 600 potentiostat) was used for maintaining the constant potential between working electrode and reference electrode thorough out the electrodeposition process. Platinum wire is used as counter electrode, Ag/AgCl as reference electrode and AAM coated with silver paste as working electrode. Silver paste coating on one side of AAM is required to make that side conducting, compulsory condition for electrodeposition to take place. Deposition of cobalt nanowires is performed at room temperature but prior to deposition the electrolytic solution was heated for some time. The electrodeposition potential was set at -0.8 V and the electrodeposition time was set for 1.5 h.

To study the in situ growth of cobalt nanowires in the pores of AAM, electrochemical impedance spectroscopic (EIS) study was done using Gamry reference 600 potentiostat. Panalytical X'PERT PRO X-Ray diffractometer with Cu- $K\alpha$ radiation was used for structural characterization of cobalt nanowires. Morphological studies were performed using JEOL JSM 6100 scanning electron microscope. I–V behaviour of cobalt nanowires was

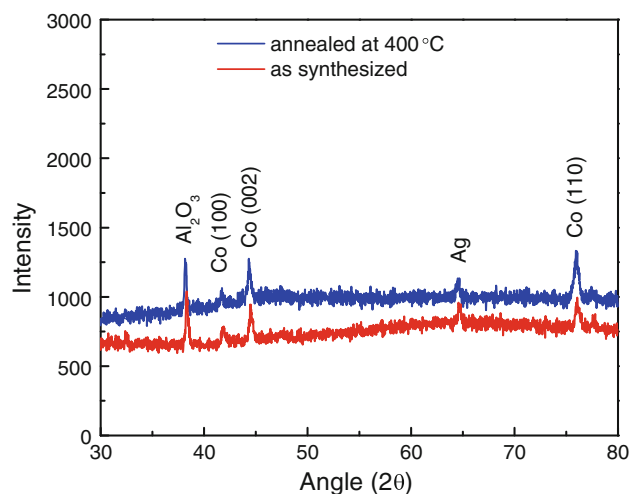


Fig. 2 X-ray diffractogram for as synthesized and annealed cobalt nanowires

investigated using Keithley 2400 source meter. Magnetic behaviour of cobalt nanowires was studied using “Quantum Design” Vibrating sample magnetometer at room temperature.

3 Results and discussion

Electrochemical impedance spectroscopy was performed during the growth process which shows the decrement in the impedance with the passage of electrodeposition time as shown in Fig. 1. Impedance diagrams in Nyquist plane clearly indicates that the high impedance of empty pores of AAM decrease with increase in cobalt metal deposition inside the pores, which diminishes as the pore is being filled. The possible equivalent circuit for the metal/AAM electrode is discussed elsewhere [17].

Figure 2 presents the X-ray diffractometer (XRD) patterns for both as synthesized and annealed cobalt nanowires in AAM. The reflection peaks in XRD patterns corresponds to hexagonal close packed (hcp) structure of cobalt nanowires with three specific peaks (100), (002) and (110). Relatively large magnitude of (002) peak, together with the absence of (101) peak clearly depicts that the c-axis of the grains within the wires is aligned parallel to the axes of the wires [19]. Some peaks due to AAM were also observed. This may be due to the fact that XRD measurements were done for cobalt nanowires embedded in the AAM. One peak corresponding to silver is also depicted from XRD patterns. This may be due to the silver paste residues after washing with acetone. X-ray diffraction pattern for as synthesized and annealed cobalt nanowires clearly depicts that the annealed sample has more prominent peaks as compared to as synthesized one and this may

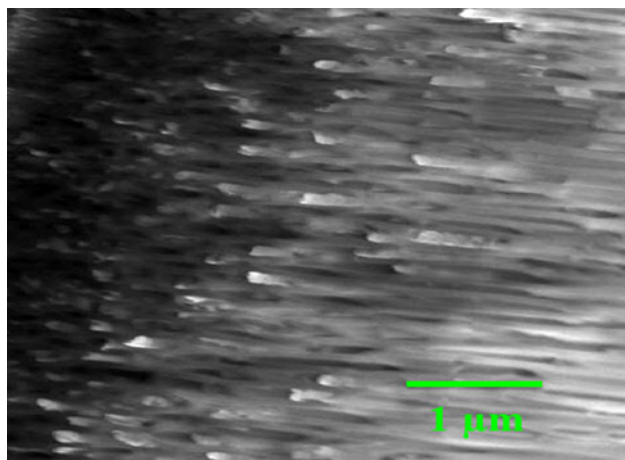


Fig. 3 SEM micrograph of cobalt nanowires in AAM

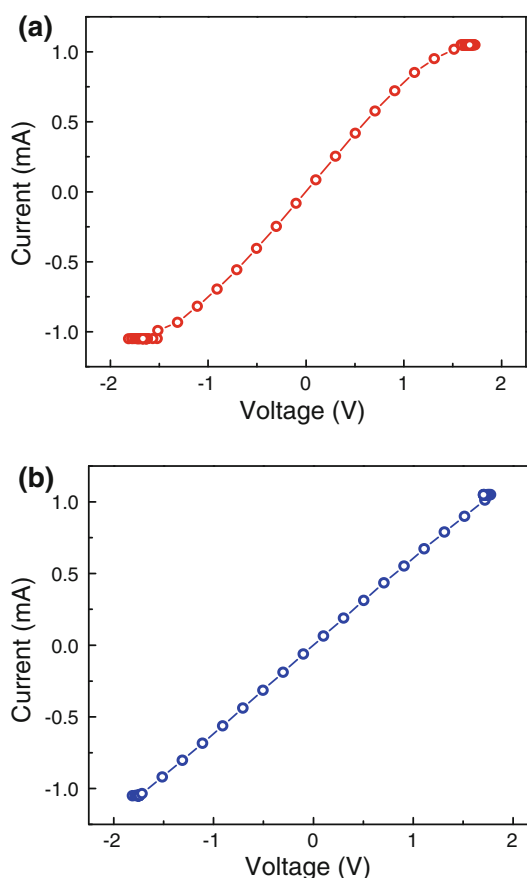


Fig. 4 **a** I–V behaviour of as synthesized cobalt nanowires in AAM. **b** I–V behaviour of cobalt nanowires annealed at 400 °C

be due to the stress relief. This indicates that the crystalline quality of cobalt nanowires is also enhanced with annealing process. Lattice parameters for cobalt nanowires calculated using Bragg's law are $a = 2.508 \text{ \AA}$ and $c = 4.090 \text{ \AA}$ for as synthesized sample and $a = 2.480 \text{ \AA}$ and $c = 4.185 \text{ \AA}$ for

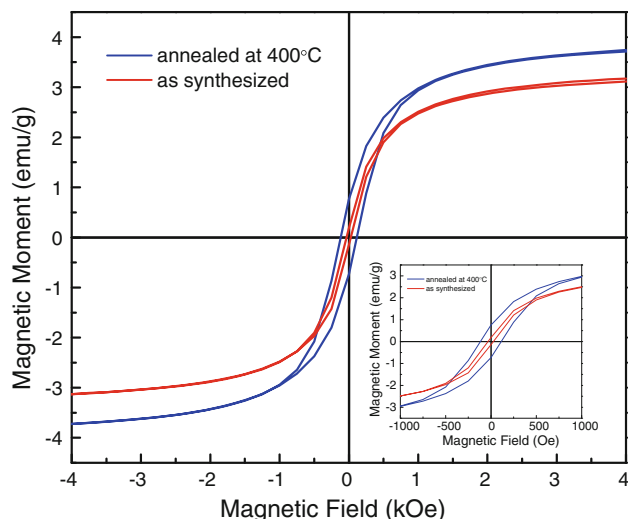


Fig. 5 M versus H curves for Co nanowires axes oriented parallel to the magnetic field

sample annealed at 400 °C. Lattice parameters are affected very little with annealing procedure [19].

Figure 3 shows the SEM micrograph of cobalt nanowires in the host AAM. It is clearly depicted from SEM micrograph that cobalt nanowires are dense and have uniform dimensions. The dimensions are almost similar to that of the pores in the AAM template. Areal density of cobalt nanowires calculated using SEM micrograph is $7 \times 10^9 \text{ cm}^{-2}$, may be an appropriate value for high density data storage.

Figure 4a, b presents the electrical (I–V) behaviour of as synthesized cobalt nanowires and annealed cobalt nanowires at 400 °C, respectively. It depicts that the current increases with increase in voltage as usually occurs in metals. But the electrical behaviour is not as simple as in bulk cobalt. Conduction is more dependent on electron scattering at the surface and grain boundaries [12–15] in the case of nanowires. Due to large surface area to volume ratio, there will be more unbounded atoms lying at the surface which further produces the defects. Because of these defects, the I–V behaviour is not linear but also contains non-linear regions too due to electron scattering (Fig. 4a). The annealing at 400 °C may reduced the defects and due to which electron scattering also decreases. Thus the increase in linearity in I–V behaviour is because of annealing process (Fig. 4b). Increase in linearity in I–V behaviour of cobalt nanowires observed due to annealing, may be useful in nanodevices.

The M (magnetization) vs H (applied field) curves for the Co nanowires embedded in AAM templates are shown in Fig. 5. The hysteresis loops were measured using a magnetic field applied parallel to the axes of the nanowires. It is clearly depicted from the inset of Fig. 5, that the

coercivity of as synthesized Co nanowires was only about 30 Oe, whereas it was observed 120 Oe for sample annealed at 400 °C. Magneto-crystalline anisotropy is mainly dominated by shape (aspect ratio) particularly in nanowires [19]. As per Stoner–Wohlfarth model, easy axis coercivity is inversely proportional to saturation magnetization [20]. One more model of reversal is proposed where coercivity falls with decreasing saturation magnetization [21]. This model was based on the consideration that the nanowires contain imperfections which reduce the local exchange. Annealing might eliminate local discontinuities in exchange coupling and so endorse coherent rotation leading to higher coercivity and support the observed experimental results. Increase in coercivity of cobalt nanowires with annealing, may be useful in data storage.

4 Conclusions

Large scale uniform Co nanowires have been synthesized in the pores of AAM template using simple and cost-effective electrodeposition technique. Using electrochemical impedance spectroscopy it was observed from the Nyquist plot, that with increase in electrodeposition time, pore resistance decreases. XRD analysis revealed the HCP structure for Co nanowires. Annealing of Co nanowires at 400 °C may reduced the defects, due to which electron scattering decreases and linearity in I–V behaviour increases. It was observed that the Co nanowires annealed at 400 °C exhibits enhanced magnetic coercivity as compared to as synthesized Co nanowires. This may be due to the reason that annealing might eliminate local discontinuities in exchange coupling leading to enhanced coercivity.

Acknowledgments This work is supported by Department of Science and Technology (DST), Govt. of India under Nano Mission scheme (sanction order no. SR/NM/NS-84/2008).

References

1. J. Topp, S. Mendach, D. Heitmann, M. Kostylev, D. Grundler, *Phys. Rev. B* **84**, 214413 (2011)
2. S.Y. Chou, M.S. Wei, P.R. Krauss, P.B. Fischer, *J. Appl. Phys.* **76**, 6673 (1994)
3. L. Carignan, V. Boucher, T. Kodera, C. Caloz, A. Yelon, D. M'énard, *Appl. Phys. Lett.* **95**, 062504 (2009)
4. D. Kaur, D.K. Pandya, S. Chaudhary, *J. Electrochem. Soc.* **159**, D713 (2012)
5. M. Almasi Kashi, A. Ramazani, M. Ghaffari, V.B. Isfahani, *J. Cryst. Growth* **311**, 4581 (2009)
6. M. Darques, A. Encinas, L. Vila, L. Piraux, *J. Phys. D Appl. Phys.* **37**, 1411 (2004)
7. M. Darques, L. Piraux, A. Encinas, P. Bayle-Guillemaud, A. Popa, U. Ebels, *Appl. Phys. Lett.* **86**, 072508 (2005)
8. Y. Ren, J. Wang, Q. Liu, Y. Dai, B. Zhang, L. Yan, *J. Mater. Sci.* **46**, 7545 (2011)
9. J.U. Cho, J.H. Wu, J.H. Min, S.P. Ko, J.Y. So, Q.X. Liu, Y.K. Kim, *J. Magn. Magn. Mater.* **303**, e281 (2006)
10. S. Ge, C. Li, X. Ma, W. Li, L. Xi, C.X. Li, *J. Appl. Phys.* **90**, 1 (2001)
11. H. Schlorb, V. Haehnel, M.S. Khatri, A. Srivastav, A. Kumar, L. Schultz, S. Fahler, *Phys. Stat. Solid B* **247**, 2364 (2010)
12. A.F. Mayadas, M. Shatzkes, *Phys. Rev. B* **1**, 1382 (1970)
13. K. Fuchs, *Proc. Camb. Phil. Soc.* **34**, 100 (1938)
14. E.H. Sondheimer, *Adv. Phys.* **1**, 1 (1952)
15. S. Kumar, A. Vohra, S.K. Chakarvarti, *Nanomater. Nanotechnol.* **2**, 1 (2012)
16. S. Kumar, D. Saini, G.S. Lotey, N.K. Verma, *Superlattice Microstruct.* **50**, 698 (2011)
17. S. Kumar, D. Saini, *Appl. Nanosci.* **3**, 101 (2013)
18. S. Kumar, D. Saini, *J. Mater. Sci. Mater. Electron.* **24**, 1086 (2013)
19. W. Li, Y. Peng, G.A. Jones, T.H. Shen, G. Hill, *J. Appl. Phys.* **97**, 34308 (2005)
20. E.C. Stoner, E.P. Wohlfarth, *Proc. R. Soc. Lond. Ser. A* **240**, 559 (1948)
21. W. Chen, S.L. Tang, M. Lu, Y.W. Du, *J. Phys. Condens. Mater.* **15**, 4623 (2003)